# On Calderón Techniques in Time Domain Integral Equation Solvers

K. Cools* F. P. Andriulli† F. Olyslager‡ E. Michielssen§

*Abstract* — **In this paper, time-domain Calderón identities will be constructed. These identities will be used in constructing a time-domain Calderón preconditioned electric field integral equation (CP-EFIE) which can be proven to be well behaved in the regime of dense discretizations. It will be explained how this modified electric field integral equation can be accurately discretized. Numerical results will be presented that compare the performance of the proposed equation and that of the classical TD-EFIE, thereby demonstrating the effectiveness of the method.**

### Introduction

Marching on in time MOT-based electric field integral equation (EFIE) solvers represent an increasingly appealing avenue for analyzing electromagnetic transients on multiscale and geometrically complex circuits and antennas. Compared to their differential equation counterparts, MOT-EFIE solvers automatically impose radiation conditions, do not require unknown fields to be discretized throughout homogeneous volumes, and are not subject to CFL conditions. Unfortunately, time-domain EFIEs discretized via marching on in time (MOT) recipes suffer from a dense-grid breakdown phenomenon whenever the time step becomes large compared to the spatial grid size. This breakdown phenomenon manifests itself in the form of ill-conditioned MOT matrices and slow convergence rates of the MOT iterative solver. The time-domain breakdown phenomenon has a direct frequency domain counterpart: frequency domain EFIEs discretized via the method of moments result in ill-conditioned matrices when the spatial grid size is small compared to the wavelength. Recently, an analytical preconditioner for the frequency domain EFIE [1, 2, 3] was developed by leveraging the Calderón identities [1]. Unfortunately, this preconditioner has no direct time-domain counterpart as it introduces extra discretization errors that more often than not trigger instabilities. Here, a preconditioner for the time-domain EFIE is developed that gives rise to an accurate stable system after discretization. To this end, the Calderón preconditioned time-domain EFIE of [4] is discretized using Buffa-Christiansen basis functions [5]. Numerical results that demonstrate the performance of the new analytical preconditioner are presented.

*Department of Information Technology (INTEC), Ghent University, Sint-Pieters Nieuwstraat 41, 9000 Gent, Belgium, e-mail: kristof.cools@intec.ugent.be, tel.: +32 9 2643353, fax: +32 9 2649969.

†Department of Electrical Engineering and Computer Science, University of Michigan, 1301 Beal Avenue, 48109 Ann Arbor, Michigan, USA, e-mail: fandri@eecs.umich.edu, tel.: +1 734 9362975, fax: +1 734 6472106.

‡Department of Information Technology (INTEC), Ghent University, Sint-Pieters Nieuwstraat 41, 9000 Gent, Belgium, e-mail: femke.olyslager@intec.ugent.be, tel.: +32 9 2643344, fax: +32 9 2649969.

§Department of Electrical Engineering and Computer Science, University of Michigan, 1301 Beal Avenue, 48109 Ann Arbor, Michigan, USA, e-mail: emichiel@umich.edu, tel.: +1 734 647 1793, fax: +1 734 6472106.

### Equations and Discretization

Consider a closed PEC surface $S$ with external normal $\hat{\boldsymbol{n}}$, that is illuminated by a transient electric field $\boldsymbol{E}^i(\boldsymbol{r},t)$. The "derivative form" of the time-domain EFIE for the current density on $S$, $\boldsymbol{J}(\boldsymbol{r},t)$, reads

$$\dot{T}\boldsymbol{J} = \dot{\boldsymbol{M}}^i. \quad (1)$$

Here $\boldsymbol{M}^i(\boldsymbol{r},t) = -\hat{\boldsymbol{n}} \times \boldsymbol{E}^i(\boldsymbol{r},t)$ represents the excitation and the operator $T$ maps $\boldsymbol{J}(\boldsymbol{r},t)$ to the trace of the scattered field $\hat{\boldsymbol{n}} \times \boldsymbol{E}^s$; $T$ can be decomposed as

$$T\boldsymbol{J} = T_h\boldsymbol{J} + T_s\boldsymbol{J} \quad (2)$$

where

$$T_s\boldsymbol{J} = -\frac{1}{c}\hat{\boldsymbol{n}} \times \int_S ds' \frac{\boldsymbol{J}(\boldsymbol{r}', t - R/c)}{4\pi R}, \quad (3a)$$

$$T_h\boldsymbol{J} = c\hat{\boldsymbol{n}} \times \int_S ds' \nabla \frac{\int_0^{t-R/c} \nabla' \cdot \boldsymbol{J}(\boldsymbol{r}', t')dt'}{4\pi R}. \quad (3b)$$

Here $H$ is the Heaviside function, $\delta$ is the Dirac impulse, and "$*$" denotes temporal convolution. The capacitive operator $T_h$ is hypersingular with a nontrivial nullspace. Discretizing equation (1) using the standard MOT recipe yields

$$\sum_{k=0}^{j-1} \mathsf{Z}^k \cdot \mathsf{I}_{j-k} + \mathsf{V}_j = 0, \quad j = 1...N_T \quad (4)$$

where $(\mathsf{Z}_k)_{m,n} = \left\langle \boldsymbol{b}'_m l'_j | \dot{T} | \boldsymbol{b}_n l_{j-k} \right\rangle$ and $(\mathsf{V}_j)_m = -\left\langle \boldsymbol{b}'_m l'_j | \boldsymbol{M}^i \right\rangle$; $\boldsymbol{b}_m$ and $\boldsymbol{b}'_n$ are spatial basis and

1-4244-0767-2/07/$20.00 ©2007 IEEE

testing functions and $l_j$ and $l'_{j-k}$ are temporal ones. Successively solving these equations for $j = 1, ..., N_T$ is equivalent to solving the lower triangular block matrix equation

$$\begin{pmatrix} \mathbf{Z}^0 & & \\ \mathbf{Z}^1 & \mathbf{Z}^0 & \\ \vdots & \vdots & \ddots \end{pmatrix} \begin{pmatrix} \mathsf{I}_0 \\ \mathsf{I}_1 \\ \vdots \end{pmatrix} + \begin{pmatrix} \mathsf{V}_0 \\ \mathsf{V}_1 \\ \vdots \end{pmatrix} = 0. \quad (5)$$

When the speed of light times the timestep is much larger than the spatial element size, the block matrix on the left side of (5) becomes ill-conditioned. In [4] the EFIE is replaced by the equation

$$\dot{T}^2 \boldsymbol{J} = \left( \dot{T}_s \dot{T}_s + \dot{T}_s \dot{T}_h + \dot{T}_h \dot{T}_s \right) \boldsymbol{J} = \dot{T} \dot{\boldsymbol{M}}^i. \quad (6)$$

The operator $T_h T_h$ is identically zero and drops out. The Calderón identities [4], show that the operator $T^2$ equals a compact perturbation of the identity $K^2 - 1/4$. This Calderón preconditioned electric field integral equation (CP-EFIE) can thus be expected to be better conditioned than the original EFIE. To arrive at a practical solution, a feasible and accurate discretization strategy for the operator $T^2$ has to be developed. This means choices for the domain and testing spaces of the left and right factors of $T^2$ have to be made. In doing so, a few rules need to be respected:

- The domain space of both factors needs to be a finite element space of divergence conforming elements, i.e. it must be possible to compute the charge distribution associated with a current distribution.
- From the operator properties of $T$ it follows that the range space of both factors needs to be a finite element space of curl conforming elements.
- It must be possible to translate an approximation of a field in the range space of the right operator into an approximation in the domain space of the left operator. In practice, this means the Gram matrix between a basis of the former space and a basis of the latter space has to be well-conditioned.

The most popular choice for a divergence conforming space of finite elements are the Rao-Wilton-Glisson basis functions. Henceforth they will be denoted as RWGd. Their curl conforming counterparts $\hat{\boldsymbol{n}} \times$ RWGd are denoted by RWGc. Using these notations, Adams [1] proposes the following discretization scheme for the frequency counterpart of equation (6):

$$\langle \text{RWGd}|T|\text{RWGc}\rangle \, \mathbf{G}^{-1} \, \langle \text{RWGc}|T|\text{RWGd}\rangle \quad (7)$$

with $\mathbf{G} = \langle \text{RWGc}|\text{RWGc}\rangle$. This scheme respects the third rule, but not the other two. To arrive at a usable solution, Adams uses a slightly different discretization for the third term in (6). Instead of the intermediate current space, the intermediate charge space is discretized. In doing so, the preconditioner becomes no longer purely multiplicative and the preconditioning process introduces extra discretization errors. In the time-domain, this error can be large enough to trigger late time instabilities. At first sight, it seems tempting to use the following scheme:

$$\langle \text{RWGc}|T|\text{RWGd}\rangle \, \mathbf{G}^{-1} \, \langle \text{RWGc}|T|\text{RWGd}\rangle \quad (8)$$

with $\mathbf{G} = \langle \text{RWGc}|\text{RWGd}\rangle$. This scheme fulfills the first two rules, but not the third. The Gram matrix between a space of divergence conforming RWG and curl conforming RWG is singular. The above reasoning explains the need for a pair of divergence and curl conforming spaces that allow an approximation by RWGc functions to be translated to an approximation in the new divergence conforming space. The Buffa-Christiansen basis described in [5] constitutes such a space. These spaces will henceforth be denoted by the symbols BCd and BCc. The most remarkable property of these spaces is that they can be expressed as subspaces of the RWG spaces defined on the barycentric refinement of the original mesh used to describe the geometry of the scatterer. In figure 1 a mesh of a sphere is plotted together with its barycentric refinement. The support of a RWG basis function and a BC basis function are indicated. The weights used in the linear combination of RWG basis functions defined on the barycentric mesh refinement are indicated in figure 2. The weights indicated on the edges that have a vertex in common with the original mesh need to be multiplied with the number indicated on this shared vertex. All RWG functions are oriented in such a way that if the support region is cycled in clockwise sense, the triangle containing the positive charge density is encountered first. Using these new spaces of finite elements, the following discretization scheme can be constructed:

$$\langle \text{BCc}|T|\text{BCd}\rangle \, \mathbf{G}^{-1} \, \langle \text{RWGc}|T|\text{RWGd}\rangle \quad (9)$$

with $\mathbf{G} = \langle \text{RWGc}|\text{BCd}\rangle$. This equation immediately reveals that the scheme obeys the first two rules. In [5], it is also proven that the Gram matrix is well conditioned. This means that the scheme also respects the third rule. Using this scheme, the

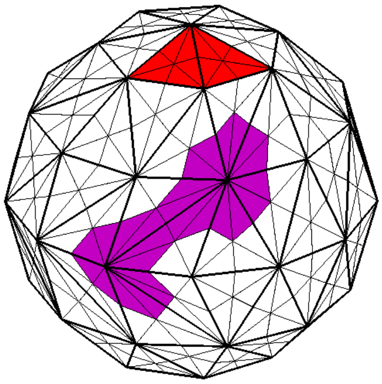

Figure 1: Example of a barycentric mesh refinement and of the support of an RWG and BC basis function respectively.

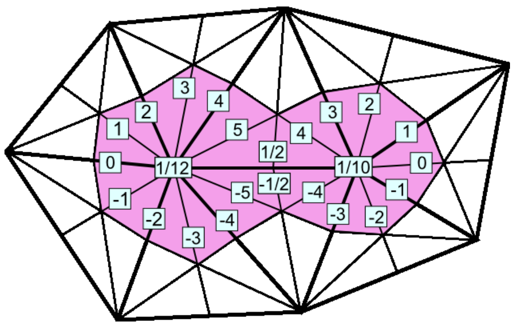


Figure 2: Weights used to construct a BC basis function as a linear combination of RWG basis functions defined on the refinement.

new MOT system is

$$0 = \begin{pmatrix} \mathbf{W}^0 & & \\ \mathbf{W}^1 & \mathbf{W}^0 & \\ \vdots & \vdots & \ddots \end{pmatrix} \cdot \mathbf{G}^{-1} \cdot \ldots$$
$$\left\{ \begin{pmatrix} \mathbf{Z}^0 & & \\ \mathbf{Z}^1 & \mathbf{Z}^0 & \\ \vdots & \vdots & \ddots \end{pmatrix} \begin{pmatrix} \mathsf{I}_0 \\ \mathsf{I}_1 \\ \vdots \end{pmatrix} + \begin{pmatrix} \mathsf{V}_0 \\ \mathsf{V}_1 \\ \vdots \end{pmatrix} \right\} \tag{10}$$

with $\mathbf{Z}^k$ and $\mathbf{W}^k$ the RWG-Galerkin and BC-Galerkin discretization of the $\dot{T}$ and $\mathbf{G}$ the Gram matrix. Also in the frequency domain, this easy to implement scheme will yield an accurate and efficient solution of PEC scattering problems.

**Numerical Results**

A sphere of radius 0.25m is discretized using different meshes with varying average edge size (see figure 3). The sphere is iluminated by a base-band

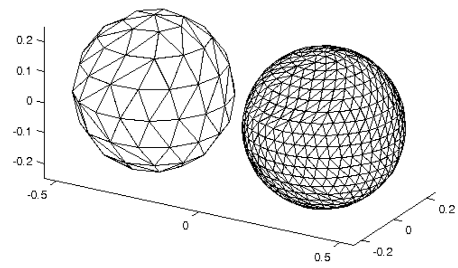


Figure 3: Coarsest and finest mesh used in the simulation of scattering by the sphere.

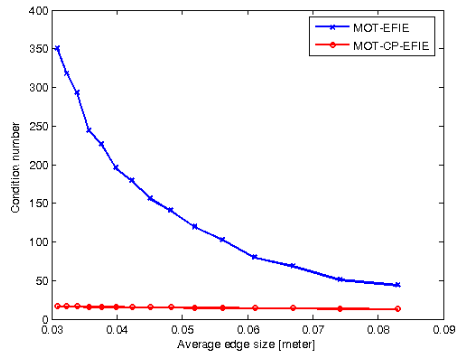


Figure 4: Condition number of the MOT-EFIE and MOT-CP-EFIE system versus the average edge size of the mesh used.

Gaussian incident wave described by the equation

$$\boldsymbol{E}^i(\boldsymbol{r}, t) = \frac{4}{T\sqrt{\pi}} \hat{\boldsymbol{x}} e^{-\gamma^2} \tag{11}$$

with $\gamma = \frac{4}{T}(ct - ct_0 - \hat{\boldsymbol{z}} \cdot \boldsymbol{r})$, $T = 8$ meter, and $t_0 = 4.00 \cdot 10^{-8}$ seconds. The time domain EFIE and CP-EFIE equations are discretized using a time step $\Delta t = 6.67 \cdot 10^{-10}$ seconds. In figure 4 the condition numbers of the resulting MOT systems are plotted versus the average edge size. It is evident from the graph that the condition number of the classical MOT-EFIE system increases with decreasing edge size. The condition of the MOT-CP-EFIE system in contrast has a constant value. In figure 5, the surface currents for the two methods are compared for an average edge size of 0.031 meter.

**References**


[1] Adams R. and Champagne N. A numerical implementation of a modified form of the electric field integral equation. *IEEE Transactions on*

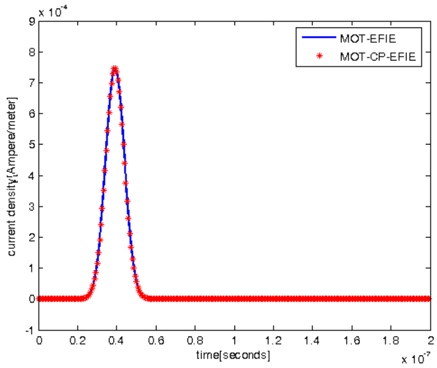


Figure 5: Comparison between the surface currents on a sphere produced by the MOT-EFIE and MOT-PC-EFIE solver respectively.

*Antennas and Propagation*, 52(9):2262–2266, september 2004.

[2] Contopanagos H., Dembart B., Epton M., Ottusch J., Rokhlin V., Visher J., and Wandzura S. Well-conditioned boundary integral equations for three-dimensional electromagnetic scattering. *IEEE Transactions on Antennas and Propagation*, 50(12):1824–1830, december 2002.

[3] S. Borel, D. P. Levadoux, and F. Alouges. A new well-conditioned Integral formulation for Maxwell equations in three dimensions. *IEEE Transactions on Antennas and Propagation*, 53(9):2995–3004, September 2005.

[4] Cools K., Andriulli F.P., and Michielssen E. Time-domain Calderón identities and preconditioning of the time-domain EFIE. *Antennas and Propagation Society International Symposium 2006, IEEE*, pages 2975 – 2978, july 2006.

[5] Buffa A. and Christiansen S. H. A dual finite element complex on the barycentric refinement. *Tech. Report PV-18 IMATI-CNR*, 2005.

FOREWORD COMMITTEES EXHIBITORS SCHEDULE SEARCH by ...

# 2007 International Conference on Electromagnetics in Advanced Applications

## ICEAA '07
## 10th Edition

September 17-21, 2007

Torino, Italy

ISBN 1-4244-0767-2